Volume 18, Number 3, 2025. pp. 319-328

Jordan Journal of Physics

ARTICLE

Heat Treatment Route Impact on 6063 Al-Mg-Si Alloy: Implications for Mechanical Properties

Mazen A. Madanat[a], **Qutaibah Al-Masri**[a], **Ayeh Arabiat**[a], **Saad S. Alrwashdeh**[b] and **Marwan S. Mousa**[c]

[a] *Metallurgy and Materials Technology Research Unit, Advanced Research Centre, Royal Scientific Society, Amman 11941, Jordan.*

[b] *Mechanical Engineering Department, Mutah University, Al-Karak 61710, Jordan.*

[c] *Department of Renewable Energy Engineering, Jadara University, Irbid 21110, Jordan.*

Doi: **https://doi.org/10.47011/18.3.6**

Received on: 10/02/2024; *Accepted on: 27/08/2024*

Abstract: The industrial 6063 Al-Mg-Si alloy was subjected to solution heat treatment, water quenching, and ageing at different heat treatment times and temperatures, such as natural ageing (NA) at room temperature, pre-ageing (PA) at elevated temperatures of 80-120 °C, and artificial ageing (AA) at 180 °C. This study investigates how clusters and precipitates formed during various ageing processes impact the mechanical properties of 6063 Al-Mg-Si alloy. The results showed that the PA temperature plays a crucial role in the formation of clusters, while AA is critical for the formation of hardening precipitates (β''). PA at ≤ 100 °C produced clusters similar to those formed during NA, while PA at 120 °C produced more stable clusters (pre-hardening precipitates) (β'' nuclei). PA followed by AA at 180 °C for 6 hours increased the hardness and the tensile strength to values similar to AA without prior PA for PA ≤ 100 °C. AA after PA at 120 °C resulted in higher values of hardness and tensile strength. A good correlation was found between Vickers hardness, yield strength, and tensile strength, which agrees with the literature.

Keywords: Natural ageing, Pre-ageing, Artificial ageing, Al-Mg-Si alloys, Mechanical properties.

Introduction

The 6xxx series aluminium alloys are widely used industrial alloys due to their formability, high strength-to-weight ratio, and corrosion resistance. The standard process for producing the alloy involves solution heat treatment (SHT) at ~540°C, followed by water quenching (WQ) to create a supersaturated solid solution (SSSS) with good formability due to its low strength. This is followed by artificial ageing (AA) at 180°C to strengthen the alloy via β'' precipitates. However, in practice, there is often an unavoidable natural ageing (NA) step at room temperature between SHT and AA. To enhance the NA effect on the AA response, two approaches have been proposed: pre-ageing (PA) and microalloying with elements such as Sn.

The addition of Sn [1–4] helps control the clustering process by binding with vacancies and facilitating precipitation during AA [5]. The PA step is applied at temperatures higher than 67°C to form PA clusters that may grow into β'' precipitates during AA. The PA temperature has been suggested [6] as a transition temperature where clusters formed at higher temperatures can only grow into β'' precipitates during AA. The effect of different PA temperatures on the

Corresponding Author: Mazen A. Madanat **Email**: madanatmazen@yahoo.com

mechanical properties of the different aluminium alloys has been studied by several researchers [1, 7–12]. In the current work, the PA effect on the 6063aluminium alloy under specific and systematic times and temperatures is presented. The term "PA clusters" is used to label clusters formed during the PA step, regardless of the different notations used for different types of clusters in the literature [13–19].

This study investigates the impact of different heat treatment routes on the mechanical properties of the 6063 alloy. In addition, the tensile properties were estimated through correlations between Vickers hardness, yield strength, and tensile strength. The different PA time and temperature have shown different effects on the mechanical properties, due to differences in cluster formation and growth within the alloy.

Materials and Methods

Industrial ternary 6063 (Al-04Mg-0.5Si-(Fe)) aluminium alloy was provided by the Arab Aluminium Industry Co. Ltd (ARAL), Jordan. Samples with dimensions of 1 × 10 × 10 mm^3 were prepared for hardness measurements. Samples were ground, polished to a mirror-like finish, and ultrasonically cleaned. Tensile samples were prepared using a CNC machine in accordance with ASTM E8 for aluminium alloys, with a gauge length of 50 mm and a width of 12.5 mm.

Solution heat treatment (SHT) was performed at 540 °C for 1 h, followed by water quenching (WQ) at room temperature. Two heat treatment routes were then applied (see Fig. 1): (A) immediate artificial ageing (AA) at 180 °C for various times, or natural ageing (NA) at room temperature for 2 weeks followed by AA; (B) immediate pre-ageing (PA) at 80-120 °C for various times, or PA followed by 2 weeks NA, or PA + 2 weeks NA followed by AA at 180 °C for 6 hours. Samples were quenched after each PA or AA step.

Tensile measurements were carried out according to the international standard ASTM E8 using a Shimadzu machine. Vickers micro-hardness measurements were performed with a load of 200 gf (HV0.2), and the average of eight indentations was used for each measurement.

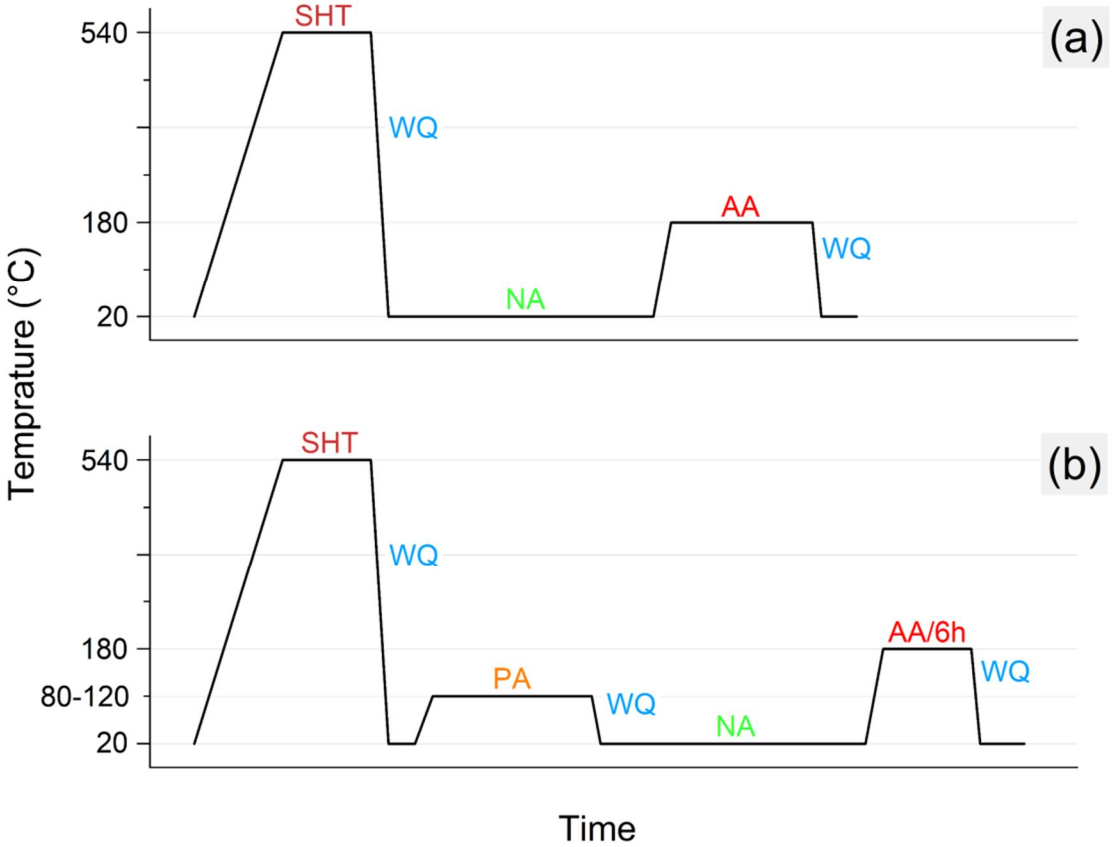

FIG. 1. Temperature profiles used in this work: (a) without PA and (b) with PA. SHT – 1 h at 540 °C, WQ at 20 °C, NA - 2 weeks at 20 °C, PA – various times at 80-120 °C, AA - various times at 180 °C in (a) and for 6 h in (b).

Results

Hardness

Figures 2(a)-2(d) present the evolution of hardness after different heat treatments. The hardness value immediately after solutionizing (SHT) and quenching (WQ) was 33 HV. Natural ageing (NA) for 2 weeks increased the hardness to 47.1 HV (red line). Artificial ageing (AA) for various times after NA reached a maximum hardness of ~88 HV after 12 hours of AA (green line). Immediate AA after SHT increased the hardness to a maximum of 61.5 HV after 8 hours of AA, but longer AA times decreased the hardness (black line). Pre-ageing (PA) at 80°C (dark blue line) and 100°C, indicated by the orange line in Fig. 2(b), showed no change in hardness up to 14 hours, while PA at 120°C (blue line) increased hardness to ~50 HV after 12 h and ~45 HV after -14 h. PA samples were then set to 2 weeks of NA, as shown in Fig. 2(c), and hardness increased to ~45 HV for the entire PA set at 100°C (orange line) and 120°C (blue line). Final AA at 180°C for 6 hours after PA and NA, illustrated in Fig. 2(d), increased the hardness to ~80 and 90 HV for PA at 100 °C and 120 °C, respectively. NA clusters retrogression or reversion was observed after AA, resulting in a slight decrease in hardness during the first minutes, due to cluster dissolution during AA [20–25].

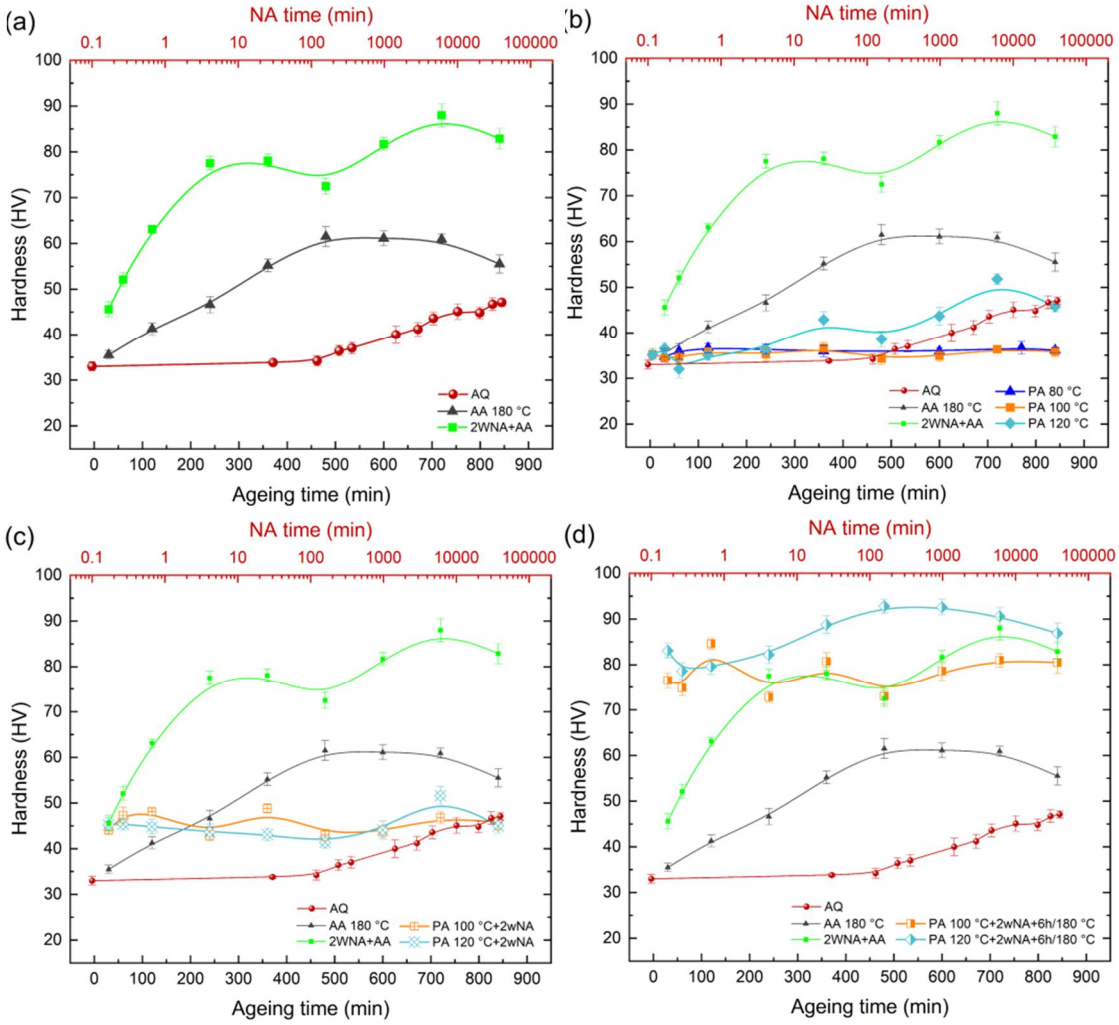

FIG. 2. Evolution of hardness (HV0.2) after different thermal treatments. The X-axis corresponds to hardness values, the upper Y-axis corresponds to NA time, and the lower Y-axis corresponds to ageing (PA or AA) times. (a–d) The red line shows the NA behavior after SHT and WQ. The black line corresponds to AA at 180°C for various times. The green line corresponds to samples subjected to NA for 2 weeks, followed by AA at 180°C for various times. (b) Hardness after PA at 80°C for various times (dark blue line), after PA at 100°C (orange line), and after PA at 120°C (blue line). (c) Hardness after PA and 2 weeks of NA. (d) Hardness after PA + 2 weeks of NA + AA at 180°C for 6 h.

Tensile measurements (PA at 120°C)

Figure 3(a) shows that the yield strength (YS) of the alloy increased from approximately 38 MPa in the AQ state to 79 MPa after 2 weeks of NA. AA at 180°C on samples that underwent NA for two weeks increased the YS from 70 MPa after 30 minutes of AA to 190 MPa after 4 hours of AA. For AA durations over 4 hours, the YS remained between 190-212 MPa up to 14 hours of AA.

PA for 30 minutes at 120°C decreased the YS to 44 MPa, but it slowly increased to 64 MPa after 6 hours of PA. The YS continued to increase and reached 104 MPa after 14 hours of PA.

2 weeks of NA after PA at 120°C showed a slight increase in the YS compared to PA without NA for PA durations up to 6 hours, with a YS of approximately 70 MPa. For longer PA durations, the YS values were similar in both cases (PA and PA + 2 weeks NA), with a maximum of 101 MPa after 14 hours of PA. Final AA after PA + 2 weeks NA affected the YS values based on the previous PA duration. PA for 4 hours or less increased the YS value to approximately 210 MPa, while PA for 6 hours or more further increased the YS value to approximately 240 MPa.

The results of the tensile strength (UTS) of the tested samples are presented in Fig. 3(b). The UTS of the AQ sample was ~118 MPa and increased to ~160 MPa after 2 weeks of NA. AA for 30 minutes resulted in a UTS of 160 MPa, which increased to a maximum of 235 MPa after 4 hours of AA. The UTS continued to increase up to 14 hours of AA. PA for 30 minutes resulted in a minimum UTS of 121 MPa, which increased to a maximum of 164 MPa after 14 hours of PA.

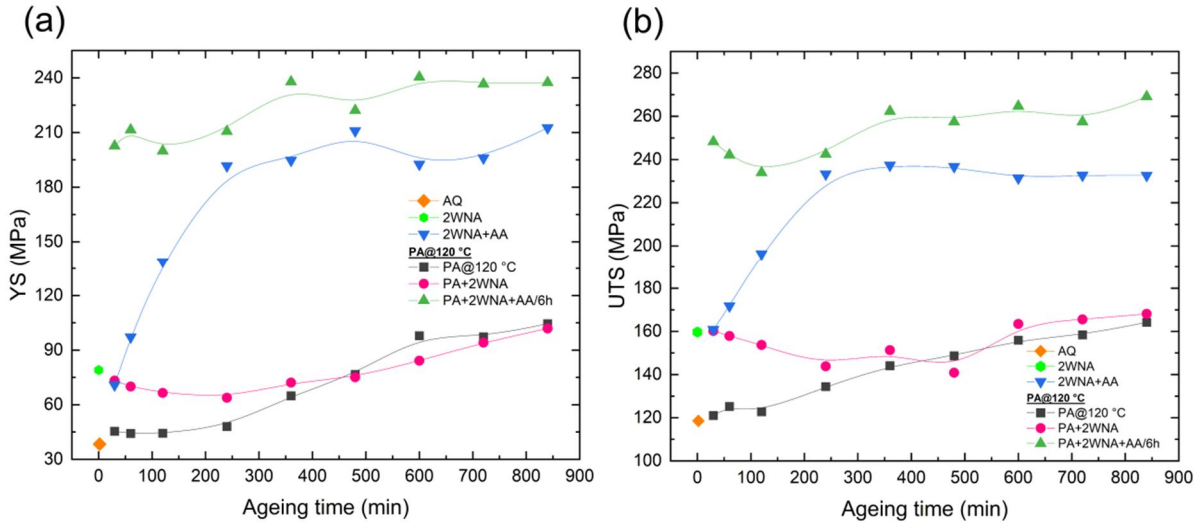

FIG. 3. (a) Evolution of yield strength (YS) and (b) ultimate tensile strength (UTS) after various heat treatment routes.

Following 2 weeks of NA after PA had a positive effect on the UTS for PA times less than 6 hours, with a UTS of 160 MPa after 30 minutes of PA and 2 weeks of NA. For PA times longer than 6 hours, the UTS values were similar for PA with and without 2 weeks of NA. Final AA at 180°C for 6 hours after PA and NA resulted in a significant increase in UTS values. AA after 30 minutes of PA and 2 weeks of NA doubled the UTS to 245 MPa. The UTS remained high at ~240 MPa for PA times up to 4 hours and had an average value of ~260 MPa for longer PA times.

Discussion

Behavior of Strength and Hardness

Without Pre-ageing

Immediately after the solution heat treatment (SHT) and quenching, a supersaturated solution forms, and solute atoms begin to diffuse and form clusters with the help of quench-in vacancies. Zurob and Seyedrezai have proposed a model for the movements of these vacancies and solute atoms [26]. They postulate that the rate of clustering is highest immediately after the SHT and quenching, due to the high concentration of mobile vacancies. The

subsequent NA process reduces the level of supersaturation and consumes vacancies until they reach thermal equilibrium, leading to slower clustering kinetics.

Figures 2(a)-2(d) depict an increase in the hardness (red curve) over 2 weeks of NA (upper Y-axis). A plateau is observed up to 120 minutes, which is linked to the size of the formed clusters. Hardness is a sensitive measure of cluster size, and a change in hardness reflects changes in the critical cluster size. In this case, the size has stabilized after 120 minutes of NA. Further increases in hardness are observed over longer NA times and have been documented by several researchers [5, 24, 25, 27–32].

Immediate AA at 180°C after quenching creates a high driving force for the solute atoms and vacancies, resulting in the formation of stable clusters and precipitates. Madanat *et al*. [27, 33] studied the impact of different heating media on Al-Mg-Si alloys immediately after quenching. They found that a shorter AA time leads to faster cluster and precipitate formation, regardless of the heating medium used. Figure 2 displays the systematic increase in the AA curve (black line). The hardness continues to increase up to a maximum after 480 minutes of AA, followed by a decrease due to over-aging and the formation of coarse precipitates. The initial increase is a result of the formation of clusters and the pre-β'' phase and the following strengthening phase β''. The final decrease is due to over-aging and the formation of β' phase.

Tensile measurements, indicated by the blue line in Fig. 3(a) and 3(b), display a systematic increase in yield strength (YS) and ultimate tensile strength (UTS), similar to the results observed in the hardness measurements. Cao *et al*. [32] used atom probe tomography (APT) to explain this behavior and found that NA alone results in a high fraction of solutes aggregating into small solute aggregates, while NA + AA leads to a slight increase in large aggregates and a good amount of small aggregates. In a recent article by Engler *et al.* [24], they reported an increase in the size of clusters and precipitates and a decrease in their number density after NA (28 days) and AA (180°C). This supports our findings, as the increase in the size of clusters and precipitates leads to an increase in hardness and strength.

With Pre-ageing

Figures 2(b)-2(d) display the hardness results after different PA treatments. Hardness changes during PA are linked to cluster formation during PA itself. According to literature, a PA temperature of 100°C is a critical temperature for cluster formation [12, 34]. Zhu *et al*. [34] reported that PA at 100°C results in low-density, small, and intermediate-sized Mg-Si co-clusters. This aligns with the tensile results shown in Figs. 3(a) and 3(b), as YS and UTS after PA have low values following PA at 100°C. For industrial use, the upper limit for YS is 130 MPa [35]. With high elongation and low strength, PA alloys exhibit low spring-back, allowing the formation of complex shapes with high dimensional accuracy during sheet metal forming processes.

The change in mechanical properties after PA is linked to cluster size. PA at 120°C for 4 hours or more increases cluster size, raising hardness. However, YS and UTS remain largely unaffected because cluster density has not yet reached an effective threshold. Hardness saturation after 10 hours at 120°C confirms this. Subsequent NA after PA can result in either new NA cluster formation or attachment to pre-existing PA clusters. Zi *et al*. [12] studied the impact of PA time and temperature on subsequent NA using resistivity, DSC, and PALS measurements. They observed an increase in resistivity during NA after PA and a dissolution trough in the DSC signal, indicating new NA cluster formation. This is consistent with other studies [6, 9, 36]. APT analysis [37] shows that cluster number density affects resistivity more than size. Researchers [10, 12] found that resistivity changes minimally after PA at 80°C and 100°C, suggesting that PA clusters grow in size rather than number. Zandbergen *et al*. [13] confirmed via APT that PA at 80°C for 2 hours increases cluster size more than density. However, [12] found that AA response is not solely improved by cluster size, indicating that other factors contribute to AA behavior after PA.

Figure 4 shows the hardening coefficient (n-values) calculated from tensile tests. The n-value indicates the material's formability and is critical to consider before the final AA step. A higher n-value corresponds to better formability (acceptable range: 0.1-0.5 [38]). The n-value is calculated from the slope of the true strength-strain curve within the plastic region using its logarithmic form.

Samples in the AQ state (Fig. 4, orange dots) and after 2 weeks of NA (Fig. 4, green dots) have high n-values of ~0.45, indicating good formability due to incomplete cluster formation. Samples after PA and PA + NA have lower n-values of ~0.38, indicating cluster formation and reduction in formability; however, they remain within the acceptable n-value limits [38, 39].

In contrast, artificial aging has a more noticeable impact as bigger clusters form. PA at 120°C reduces the n-value to ~0.38 (Fig. 4, black curve), while PA + 2 weeks NA (Fig. 4, pink curve) slightly increases the n-value. PA stabilizes clusters during subsequent NA, thus the formability (n-value) is expected to be similar.

The increase in hardness after AA is shown in Fig. 2(a), whereas the corresponding increase in strength is shown in Figs. 3(a) and 3(b). The effect of prior PA and NA is evident, with a greater increase in values seen in samples with prior PA. The formation of clusters and precipitates requires vacancies, and a reduction in vacancy concentration after PA and NA is noted. According to Pogatscher *et al.* [21], the quenched-in vacancies play a critical role in the formation of clusters and precipitates after AA. The authors argue that most of the excess quenched-in vacancies from the PA step should be either annihilated or trapped, leaving only mobile thermal equilibrium vacancies. After AA at 180°C, there will be a new and higher equilibrium vacancy concentration, which is estimated to equilibrate in about 1 minute or less [42, 43]. Thus, the PA temperature is not a factor in this process.

In such a case, it is likely that the Mg:Si ratio of clusters formed at higher PA temperature (120°C in this case) is closely related to the strengthening precipitates (β'' nuclei), enabling their easy transformation into fully coherent β'' phase upon AA. This explains the observed high hardness, YS, UTS, and low n-values after AA with a prior short PA time (30 min).

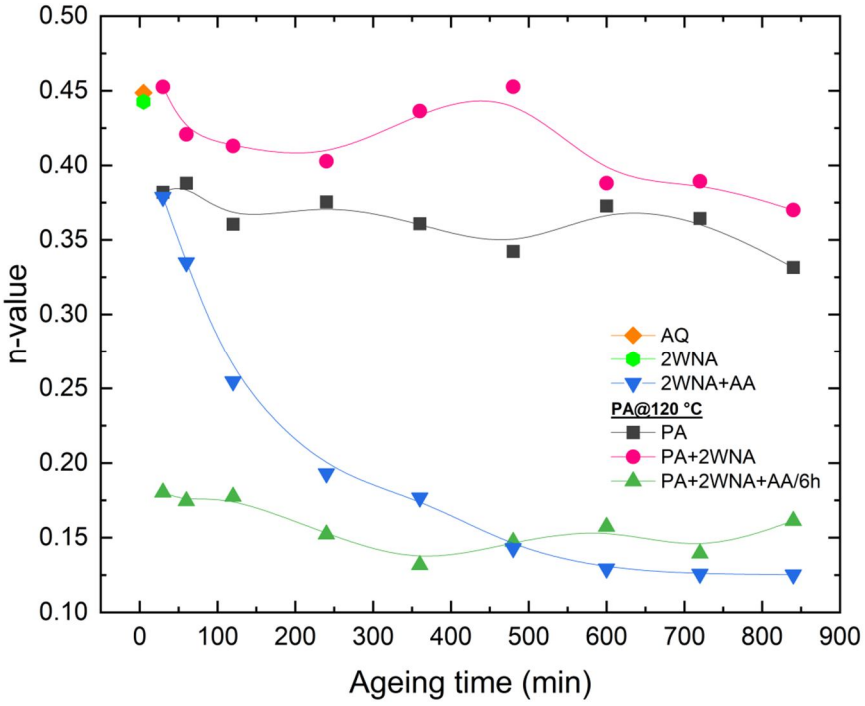

FIG. 4. Evolution of n-value before and after PA at 120°C for various times.

The chemical composition of clusters and precipitates, particularly their Mg:Si ratio, is critical in determining the outcome of heat treatment [13, 15, 23, 40, 41]. Clusters with higher Mg:Si ratios are favored at elevated temperatures [13]. These clusters are more ordered, which facilitates their transformation into β''-type strengthening precipitates during AA.

Consequently, performing PA at 100°C or 120°C leads to an increase in hardness and YS after a subsequent NA step, as the Mg:Si ratio approaches a critical value. Subsequent AA further enhances hardness and YS. Among these conditions, PA at 120°C produces the highest AA response, indicating the formation of clusters

with a higher Mg:Si ratio, closer in composition to the β''-phase.

Short preliminary annealing times lead to the formation of more clusters, while longer annealing times result in the growth of both cluster size and chemical composition. In this study, no change in hardness was observed at 80°C and 100°C after up to 14 hours of PA, while at 120°C, the hardness increased with increasing PA time. After approximately 10 hours of PA, the hardness stabilized, indicating that the critical size and chemical composition had been reached.

Correlation between Strength and Hardness

Determining yield strength and tensile strength from hardness measurements is of significant interest.

The Vickers hardness (HV) is calculated by dividing the applied load by the contact area under the indenter, resulting in a relationship with the mean pressure under the indenter (P_m). This relationship can be expressed as:

$$HV = 0.927 \cdot P_m \quad (1)$$

where $P_m = C \cdot \sigma_Y$ (2)

where σ_Y represents the tensile yield strength and HV is the Vickers hardness in MPa. The constraint factor, C, has been extensively studied by various researchers [42–45] with values ranging from 2.8 to 3. These values apply to materials that have undergone full hardening. In our study, the alloy was pre-aged (at 120°C), which strongly suppressed work hardening; thus, we assumed a fully hardened alloy and used C = 3 for comparison purposes.

By combining Eqs. (1) and (2) we get:

$$\sigma_Y = \frac{H_V}{0.927 \cdot C} \quad (3)$$

After rearranging Eq. (3) to calculate the slope,

$$\frac{\sigma_Y}{HV} = \frac{1}{0.927 \cdot C} \quad (3.1)$$

By using C = 3, the slope is equal to $\frac{\sigma_Y}{HV} = 0.365$

Experimentally, the relationship between the Vickers hardness and tensile yield strength was found to be described by a linear fit with the equation:

$$\sigma_Y = \beta_1 \cdot HV + \beta_0 \quad (4)$$

where β_1 is the slope and β_0 is the Y-intercept.

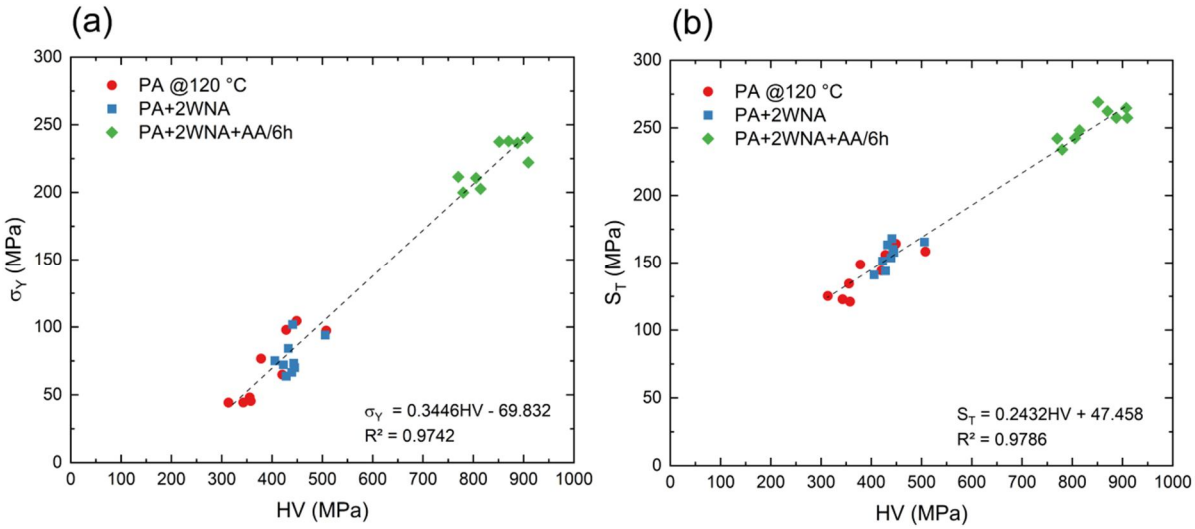

FIG. 5. Vickers hardness versus (a) yield strength and (b) tensile strength for samples investigated in this work after PA at 120°C. In this work, Vickers hardness is reported in MPa, which is found by multiplying the traditional Vickers number by the gravitational acceleration.

Figure 5(a) shows the relation between yield strength and hardness measurements. Applying a linear fit, Eq. (4) can be found as:

$$\sigma_Y = 0.345HV - 69.8 \quad (4.1)$$

The slope value of 0.345 is closely aligned with the calculated and literature value of 0.365, with a high coefficient of determination R^2 = 0.974. Tiryakioglu [44] attributed the negative y-intercept to the increase in strength under the indenter, resulting from work hardening, until it reaches the characteristic strain in the Vickers hardness test.

On the other hand, Fig. 5(b) shows the relation between Vickers hardness and tensile strength. The linear fit line has the equation:

$$S_T = 0.243HV + 47.5 \quad (4.2)$$

The R^2 shows a value of 0.979 with a slope equal to 0.243, which is similar to the value of 0.247 for alloy 7010 reported in literature [44].

In conclusion, Eqs. (4.1) and (4.2) provide the relationship between Vickers hardness and tensile yield strength, and between hardness and tensile strength, respectively.

In summary, the final mechanical properties are not only related to the final AA step but also to the earlier aging steps, namely the PA and NA. The AA after PA leads to an increase in strength due to clusters and precipitate formation, where the PA temperature is critical. PA at 120°C affects the size, density, and chemical composition of clusters, which, after subsequent AA, produce the strongest ageing response, resulting in increased strength and hardness.

Conclusion

In this study, a combination of hardness and tensile measurements was performed to examine the behavior of the age-hardening 6063 aluminum alloy in industrial applications under various thermal treatments. Samples were subjected to heat treatment at different durations and temperatures. The results indicated that:

- The pre-aging and natural aging significantly affect the alloy's mechanical and chemical properties.
- A critical PA temperature is required before the final AA step to achieve the desired microstructure.
- Pre-aging prior to natural aging has a positive effect on the alloy, as strength increases after pre-aging and aging.
- Pre-aging at 120°C is required for enhancing the final mechanical properties of the alloy by the formation of stable clusters (β'' nuclei), which transform into fully coherent hardening precipitates (β'') during subsequent aging.
- The relationship between Vickers hardness and yield strength is given by: $\sigma_Y = 0.345\,HV - 69.8$, with a slope of 0.345 closely matching literature values using a constraint factor of 3. Meanwhile, the relationship between hardness and tensile strength is: $S_T = 0.243HV + 47.5$.

Future work

Future studies will explore more complex heat treatment routes, including combinations of PA, NA, and AA, on the same alloy as well as on different alloys to determine the optimal heat treatment route with minimal energy requirements and optimal mechanical properties.

Acknowledgment

The authors would like to thank the Arab Aluminium Industry Co. Ltd (ARAL) for providing the alloy for this work.

This research did not receive any specific grant from funding agencies in the public, commercial, or not-for-profit sectors.

CRediT

Mazen Madanat: Conceptualization, Data curation, Formal analysis, Writing - original draft; Writing - review & editing, Supervision; *Qutaibah Al-Masri:* Experimental work, Data curation, Formal analysis; *Ayeh Arabiat:* Experimental work, Data curation, Formal analysis; *Saad S. Alrwashdeh:* Writing - review & editing; *Marwan S. Mousa:* Writing - review & editing.

Data Availability

The data that support the findings of this study are available from the corresponding author upon reasonable request.

References

[1] Zhang, X., Liu, M., Wang, J., Li, J., and Banhart, J., J. Mater. Sci., 57 (2022) 2149.

[2] Zhang, X., Liu, M., Sun, H., and Banhart, J., Materialia, 8 (2019) 100441.

[3] Schmid, F., Uggowitzer, P.J., Schäublin, R., Werinos, M., Ebner, T., and Pogatscher, S., Materials, 12 (11) (2019) 1801.

[4] Liu, M. *et al*., Materialia, 6 (2019) 100261.

[5] Pogatscher, S. *et al*., Appl. Phys. Lett., 112 (2014) 225701.

[6] Saga, M., Sasaki, Y., Kikuchi, M., Yan, Z., and Matsuo, M., Mater. Sci. Forum, 217 (1996) 821.

[7] Zhen, L. and Kang, S.B., Scr. Mater., 36 (10) (1997) 1089.

[8] Zhen, L., Kang, S.B., and Kim, H.W., Mater. Sci. Technol., 13 (11) (1997) 905.

[9] Birol, Y., Mater. Sci. Eng. A, 391 (1–2) (2005) 175.

[10] Ding, L., Weng, Y., Wu, S., Sanders, R.E., Jia, Z., and Liu, Q., Mater. Sci. Eng. A, 651 (2016) 991.

[11] Takaki, Y., Masuda, T., Kobayashi, E., and Sato, T., Mater. Trans., 55 (8) (2014) 1257.

[12] Yang, Z., Liang, Z., Leyvraz, D., and Banhart, J., Materialia, 7 (2019) 100413.

[13] Zandbergen, M.W., Xu, Q., Cerezo, A., and Smith, G.D.W., Acta Mater., 101 (2015) 136.

[14] Zandbergen, M.W., Cerezo, A., and Smith, G.D.W., Acta Mater., 101 (2015) 149.

[15] Serizawa, A., Hirosawa, S., and Sato, T., Metall. Mater. Trans. A, 39A (2008) 245.

[16] Edwards G.A., Stiller, K., Dunlop, G.L., and Couper, M.J., Acta Mater., 46 (11) (1998) 3893.

[17] Murayama, M. and Hono, K., Acta Mater., 47 (5) (1999) 1537.

[18] Marioara, C.D., Andersen, S.J., Jansen, J., and Zandbergen, H.W., Acta Mater., 51 (3) (2003) 789.

[19] Banhart, J., Chang, C.S.T., Liang, Z.Q., Wanderka, N., Lay, M.D.H., and Hill, A.J., Adv. Eng. Mater., 12 (7) (2010) 559.

[20] Gupta, A.K., Lloyd, D.J., and Court, S.A., Mater. Sci. Eng. A, 301 (2) (2001) 140.

[21] Pogatscher, S., Antrekowitsch, H., Leitner, H., Ebner, T., and Uggowitzer, P.J., Acta Mater., 59 (9) (2011) 3352.

[22] Yan, Y., Liang, Z.Q., and Banhart, J., Mater. Sci. Forum, 794–796 (2014) 903.

[23] Aruga, Y., Kozuka, M., Takaki, Y., and Sato, T., Mater. Sci. Eng. A, 631 (2015) 86.

[24] Engler, O., Marioara, C.D., Aruga, Y., Kozuka, M., and Myhr, O.R., Mater. Sci. Eng. A, 759 (2019) 520.

[25] Liu, M., Čížek, J., Chang, C.S.T., and Banhart, J., Acta Mater., 91 (2015) 355.

[26] Zurob, H.S. and Seyedrezai, H., Scr. Mater., 61 (2) (2009) 141.

[27] Madanat, M., Liu, M., Zhang, X., Guo, Q., Čížek, J., and Banhart, J., Phys. Rev. Mater., 4 (6) (2020) 063608.

[28] Yang, Z. *et al*., Scr. Mater., 190 (2021) 179.

[29] Yang, Z. and Banhart, J., Acta Mater., 215 (2021) 117014.

[30] Dumitraschkewitz, P., Gerstl, S.S.A., Stephenson, L.T., Uggowitzer, P.J., and Pogatscher, S., Adv. Eng. Mater., 20 (10) (2018) 1800255.

[31] Tu, W. *et al*., Mater. Des., 198 (2021) 109307.

[32] Cao, L., Rometsch, P.A., and Couper, M.J., Mater. Sci. Eng. A, 571 (2013) 77.

[33] Madanat, M.A., Ph.D. thesis, Technische Universität Berlin, Germany, (2018).

[34] Zhu, S., Shih, H.-C., Cui, X., Yu, C.-Y., and Ringer, S.P., Acta Mater., 203 (2021) 116455.

[35] Kleiner, S., Henkel, C., Schulz, P., and Uggowitzer, P.J., Int. Aluminium J., 77 (3) (2001) 185.

[36] Panseri, C. and Federighi, T., Acta Metall. Mater., 8 (4) (1960) 217.

[37] Esmaeili, S., Vaumousse, D., Zandbergen, M.W., Poole, W.J., Cerezo, A., and Lloyd, D.J., Philos. Mag., 87 (25–27) (2007) 3797.

[38] Prillhofer, R., Rank, G., Berneder, J., Antrekowitsch, H., Uggowitzer, P.J., and Pogatscher, S., Materials, 7 (7) (2014) 5047.

[39] Castany, P., Diologent, F., Rossoll, A., Despois, J.-F., Bezençon, C., and Mortensen, A., Mater. Sci. Eng. A, 559 (2013) 558.

[40] Aruga, Y., Kim, S., Kozuka, M., Kobayashi, E., and Sato, T., Mater. Sci. Eng. A, 718 (2018) 371.

[41] Torsaeter, M. et al., J. Appl. Phys., 108 (7) (2010).

[42] Shield, R.T., Proc. R. Soc. Lond. A., 233 (1193) (1955) 267.

[43] Shaw, M.C. and DeSalvo, G.J., J. Eng. Ind., 92 (2) (1970) 480.

[44] Tiryakioğlu, M., Robinson, J.S., Salazar-Guapuriche, M.A., Zhao, Y.Y., and Eason, P.D., Mater. Sci. Eng. A, 631 (2015) 196.

[45] Tabor, D., Proc. R. Soc. Lond. A, 192 (1029) (1948) 247.